DYNAMIC COMPENSATION AND FORCE CALIBRATION TECHNIQUES FOR A STATIC AND DYNAMIC THRUST MEASUREMENT SYSTEM

F. L. Crosswy and H. T. Kalb

ARO, Inc.

November 1968

ARNOLD ENGINEERING DEVELOPMENT CENTER
AIR FORCE SYSTEMS COMMAND
ARNOLD AIR FORCE STATION, TENNESSEE

NOTICES

DYNAMIC COMPENSATION AND FORCE CALIBRATION TECHNIQUES FOR A STATIC AND DYNAMIC THRUST MEASUREMENT SYSTEM

F. L. Crosswy and H. T. Kalb

ARO, Inc.

FOREWORD

The work presented herein was sponsored by Headquarters, Arnold Engineering Development Center (AEDC), Air Force Systems Command (AFSC), Arnold Air Force Station, Tennessee, under Program Element 62302F, Project 5730, Task 04.

The results of the research presented were obtained by ARO, Inc. (a subsidiary of Sverdrup & Parcel and Associates, Inc.), contract operator of the AEDC under Contract F40600-69-C-0001. The research and testing were conducted from June to August 1967 under ARO Project No. BC5820, and the manuscript was submitted for publication on August 19, 1968.

This technical report has been reviewed and is approved.

Forrest B. Smith, Jr.
Research Division
Directorate of Plans
  and Technology

Edward R. Feicht
Colonel, USAF
Director of Plans
  and Technology

ABSTRACT

An electrodynamic actuator and a solenoid-driven impact device
were used separately for dynamic force excitation of an experimental
thrust stand. Electronic compensation techniques were used to eliminate
load cell signal distortions caused by the dynamic-force-induced transient
response characteristics of the thrust stand structure. It was determined
that proper compensation circuit adjustments could be made when using
either the electronically and mechanically simple impact device or the
more complex actuator. For the conditions of this particular study,
identical dynamic force measurement accuracies were possible following
either of two procedures, (1) dynamic time domain force calibration
with the electrodynamic actuator or (2) dynamic compensation adjustments
with dynamic force excitation furnished by the impact device followed by
a static deadweight force calibration.

CONTENTS

APPENDIX
Illustrations

NOMENCLATURE

ζ Damping ratio

ω_n Undamped natural frequency

ω_o Damped natural frequency

SECTION I
INTRODUCTION

1.1 THE DYNAMIC THRUST MEASUREMENT PROBLEM

The solution to the dynamic thrust measurement problem is the realization of a measurement system which produces an electrical analog signal with an instantaneous tracking error percentage as small as possible. Instantaneous tracking error percentage is defined at any instant of time as:

$$\frac{(\text{Actual Input Force} - \text{Measurement System Indicated Force}) \times 100 \text{ Percent}}{\text{Actual Input Force}} \qquad (1)$$

In general, rapidly changing thrust forces will excite the structural natural frequencies of the thruster and thrust stand, which could result in large instantaneous tracking errors. However, several techniques may be used to reconstruct an accurate analog representation of the thrust force.

The so-called reaction force summation or accelerometer compensation technique is directly applicable for compensation of distorted load cell data caused by single-degree-of-freedom dynamic response of a thruster-thrust stand structure (Refs. 1 through 4). Also, this technique inherently possesses the valuable asset of insensitivity to thrust butt motions. This means that distortion of the thrust measurement signal because of thrust butt motions attributable to thrust inputs or test cell vibrations can be greatly reduced as compared with the conventional measurement system. However, this technique can compensate for only one natural frequency of the thruster-thrust stand structure. The first mode natural frequency of a typical thruster-thrust stand structure is usually compensated. However, the differentiating nature of the accelerometer signal will result in amplification of the higher mode natural frequency signals, and large instantaneous tracking errors may again result.

Another technique which can be used to compensate for the natural frequency distortions of a thrust stand is the so-called computer compensation technique. The phrase "computer compensation technique" gives a somewhat limited description of this compensation technique since passive circuitry could be used as well as analog computer-type circuitry. However, use of analog operational amplifier circuitry is the more versatile and economical approach. Regardless of the actual electronic components used, the compensation method depends upon

1

operation on the distorted thrust data by an electronic circuit which possesses the inverse transfer function of the thruster-thrust stand structure. The thrust information is distorted by the transfer function of the thrust stand structure and reconstructed by the compensator circuitry. A thrust measurement system using this technique is susceptible to data distortion by thrust butt motions - a disadvantage as compared with the reaction force summation technique. However, the computer compensation technique can be used to compensate for multidegree-of-freedom response of the thruster-thrust stand structure.

The combination of the unique properties of the reaction force summation technique (insensitivity to thrust butt motions) and the computer compensation technique (capable of compensating for multidegree-of-freedom response of the thruster-thrust stand) results in a versatile "hybrid" dynamic thrust measurement system (Refs. 3 and 4). A hybrid thrust measurement system was used to record all data presented in the following sections.

1.2 DYNAMIC FORCE CALIBRATION

The validity and accuracy of a particular dynamic thrust measurement technqiue must finally be proved by comparison of the measurement system output signal with an analog signal representative of a known dynamic input force.

The electrodynamic actuator is a device which can conveniently be used to generate dynamic forces. The actuator output force is directly proportional to and in time phase with the armature current, provided the static magnetic field is held constant. The force-to-armature current calibration can be effected in a straightforward manner by deadweight loading. After calibration the actuator armature can be driven by a current function generator to produce variable-frequency sinusoidal or complex time-dependent current waveforms. An analog presentation of the actuator armature current is then a direct indication of the instantaneous force level. Actuator excitation of the thrust stand with sinusoidal forces permits an evaluation of stand dynamic response characteristics in the frequency domain. Time domain specification of the thrust stand instantaneous tracking error characteristics is possible when the actuator armature is driven by a current waveform approximating the expected rocket thrust function. The electrodynamic actuator, coupled with a properly designed current function generator and static deadweight force calibrator, has been found to be a valuable dynamic force calibrator (Refs. 3 and 4).

2

During a previous study (Ref. 4), it was determined that the instantaneous force, at the 50-lb level, delivered by the electrodynamic actuator could be determined to within two percent of the actual force when using oscilloscope photographs to record the data. The largest portion of this error, 1.3 percent, was caused by the resolution error of the oscilloscope presentation. The remaining error consisted of the random error of the actuator deadweight calibration and the error caused by inductive voltage drops across the current shunt in the actuator armature circuit.

In spite of its desirable characteristics, the use of an electrodynamic actuator dynamic force calibrator adds significantly to the mechanical complexity of a thrust stand. The cost of a complete electrodynamic actuator-type dynamic force calibration system is also a significant consideration. The operation of the actuator at high force levels also introduces an appreciable damping force during calibration which does not exist during engine operation. Therefore, dynamic compensation adjustments effected during dynamic force calibration are slightly in error during the actual test. For these reasons, a more simple and less expensive impact-type dynamic force exciter and static deadweight force calibrator combination was experimentally evaluated as a possible substitute for the electrodynamic actuator dynamic force calibrator.

For the particular experimental thrust stand shown in Fig. 1 (Appendix), it will be shown in the following sections that excitation of the force column natural frequencies by periodic impact of a solenoid-driven steel rod is sufficient to allow accurate adjustment of the dynamic compensation circuits. This compensation procedure followed by a static deadweight force calibration permits as accurate dynamic force measurements as when the force measurement system is calibrated with the electrodynamic actuator dynamic force calibrator.

SECTION II
APPARATUS

2.1 EXPERIMENTAL THRUST STAND

The single-axis experimental thrust stand used to evaluate the "hybrid" thrust measurement technique, the electrodynamic actuator dynamic force calibrator, and the solenoid exciter, is shown in Fig. 1. The force column of the stand consists of the armature of an electrodynamic actuator, an accelerometer housing and a thrust butt-mounted load cell. Static deadweight calibration forces are imparted to the force column with a cable and low-friction bearing assembly.

3

2.2 ELECTRODYNAMIC ACTUATOR

An electrodynamic actuator is used to impart static and dynamic forces to the force column of the thrust stand. The actuator output force is given by

$$\bar{F}(t) = n\, I(t)\, \bar{L} \times \bar{B} \tag{1}$$

where $\bar{F}(t)$ is the time-dependent actuator vector force, $I(t)$ is the time-dependent armature current, $\bar{L}$ is the spatial orientation of the armature coils, n is the number of armature coils, and $\bar{B}$ is the field strength of the actuator magnetic field. From Eq. (1) it can be seen that for a constant magnetic field strength, the actuator output force is directly proportional to and in phase with the armature current.

A variable amplitude, variable rise and fall time current ramp function generator is used to drive the actuator armature. The current function generator can be programmed to produce a force-time function approximating rocket thrust rise time, burn time, and tailoff. A block diagram of the current function generator and electrodynamic actuator is shown in Fig. 2. A low ohmic resistance current shunt, fabricated with a low temperature coefficient of resistivity metal alloy, is included in the armature electrical circuit to produce a voltage proportional to armature current. The current shunt is geometrically constructed to minimize inductive voltage drops during periods of rapidly changing armature currents. The inductance of the presently used shunt is $0.15\ \mu h$, and inductive voltage drops are a small percentage of the shunt signal. Typical waveforms taken from the current shunt are shown in Fig. 3, where the variable rise and fall time capabilities of the current function generator are illustrated.

The generator is capable of producing preselected linear current rise times from 0.5 to 20 msec, constant level current flow from 25 to 300 msec, and current fall times from 0.6 to 20 msec. The maximum current amplitude is variable from 0 to 12 amp, giving a peak force range from 0 to 75 lb.

Fast rise and/or fall time forces produced by the actuator excite the natural frequencies of the force column. These natural frequency distortions appear in the load cell signal and are then eliminated by proper adjustments of the electronic compensation circuits of the hybrid force measurement system. Simultaneous oscilloscope presentation of the actuator force analog signal (the current shunt voltage) and the hybrid force measurement system signal permits a direct evaluation of the instantaneous tracking error characteristics of the force measurement system. This procedure constitutes a time-domain dynamic force calibration of the force measurement system.

4

Abrupt current changes in the actuator armature electrical circuit produce an appreciable inductive voltage drop in the armature circuit and induce an appreciable voltage in the static magnetic field electrical circuit. Motion of the armature coils with respect to the static magnetic field generates a back electromotive force. These phenomena oppose the desired control of the actuator armature current by the function generator. However, the differential error control amplifier circuitry of the function generator possesses sufficient response characteristics to perform high-speed corrections with the result that precisely controlled armature currents are possible. Induced voltages produced in the magnetic field coils, because of changing armature currents, can result in appreciable field currents and, therefore, distort the desired force-time function. The effects of these induced voltages are practically eliminated by current control circuitry similar to that used for armature current control and by operation of the static magnetic field in the saturation region of its magnetization characteristic. However, precise control of the armature and magnetic field currents is accompanied by several somewhat undesirable features.

The circuitry necessary to maintain precise control of the armature and magnetic field currents is moderately complex, but a more undesirable feature is dissipation of mechanical energy caused by the armature current control circuitry. With the force column at rest, the initial energy required to force current through the armature coils is totally furnished by the electrical power supply of the current function generator. Subsequent vibratory motion of the armature coils with respect to the static magnetic field results in the availability of electrical energy because of the mechanical motion. Part of the total electrical energy required to produce the desired force is now furnished by the motion of the force column. This series of events results in dissipation of mechanical energy or damping. Electronic adjustments are set into the hybrid force measurement system on the basis of force column motions under the influence of the force and damping conditions dictated by the electrodynamic actuator. These electronic adjustments will be slightly in error during the actual rocket firing since the actuator damping action will not be effective during the test. Experience has shown that the effect of the damping action of the actuator is small but not entirely negligible. The damping ratio, ζ, of the system shown in Fig. 1 is 0.004 during free vibration of the force column, whereas ζ, is about 0.018 when the motion is damped by the actuator.

The actuator can also be driven with sinusoidal current waveforms. This allows determination of the dynamic response characteristics of the thrust measurement system in the frequency domain.

2.3 SOLENOID EXCITER

Experience has shown that the dynamic compensation adjustments of the hybrid system could be accurately and quite simply effected by use of a solenoid-type impact device. The solenoid exciter system consists of a solenoidal magnetic field winding, a resilient material-tipped metal plunger, and an electronic current pulsing circuit. A diagram of the exciter system is shown in Fig. 4. The pulser furnishes impact and retract current pulses to the magnetic field windings. The periodic impact current pulses produce a magnetic field which causes the plunger to impact upon point A of the experimental thrust stand (Fig. 1). The periodic retract current pulses produce a magnetic field which returns the plunger to its initial position. The peak impact force and force rise time are controlled by the impact current magnitude and by the thickness and impact properties of the particular resilient material used to tip the plunger. Peak impact forces of several hundred pounds are easily attained.

The solenoid exciter is a simple, rugged device and is inherently compatible with the vacuum environment of a rocket test cell. The use of a solenoid exciter does not add significantly to the mechanical complexity of a thrust stand. With slight mechanical modifications, existing conventional thrust stands could utilize the solenoid exciter and hybrid thrust measurement techniques to effect dynamic as well as static thrust measurements.

The integration of an electrodynamic actuator into a dynamic thrust stand requires great care in the alignment of the armature with respect to the static magnetic field structure. Clearance between the armature and field structure is of the order of 0.020 in. Mechanical contact of the armature and field structure can result in destruction of the actuator. Multiaxis thrust measurement systems would be severely restricted by the alignment requirements imposed by an electrodynamic actuator placed in the principal thrust axis. On the other hand, the alignment requirements of the solenoid exciter are not at all critical.

The simple solenoid exciter used in the present study did not produce an analog signal proportional to its impact force. It was used solely to excite the force column natural frequencies so that the hybrid thrust measurement system circuits could be adjusted. However, it would not be particularly difficult to fabricate a solenoid plunger or pivoted impact device using a dynamic force gage. The dynamic force gage impact device would then produce an electrical signal proportional to the impact force and could conceivably be used as a dynamic force calibrator. The force gage impact device concept is shown in Fig. 5.

6

The use of the solenoid exciter to make the dynamic compensation adjustments is discussed in Section IV.

2.4 FORCE MEASUREMENT SYSTEM INSTRUMENTATION

A block diagram of the instrumentation for the hybrid, static and dynamic force measurement system is shown in Fig. 6. The basic transducer is a conventional load cell with a maximum force rating of 500 lb. Load cell electrical excitation is furnished by a conventional voltage-regulated power supply. The accelerometer is an undamped piezoelectric type with a mounted resonant frequency of 27,000 Hz. The accelerometer signal is led to a conventional charge amplifier, which in turn furnishes one input signal to the summing amplifier. The load cell signal furnishes the other signal to the summing amplifier. The output of the summing amplifier furnishes the input signal to the linear phase filter, which is a Bessel type with a variable cutoff frequency (100 to 10,000 Hz) and an attenuation rate of 18 db per octave. The computer compensator is an approximate differentiator type (Ref. 3) with a natural frequency compensating range from 20 to 2,000 Hz and a damping ratio compensating range from zero to 1.0. The gain amplifiers and the summing amplifier are formed from conventional operational amplifiers with a unity gain-bandwidth product of 2 MHz. The digital voltmeter has an ultimate resolution of 1 mv. The null indicating voltage standard has an ultimate resolution of 20 μv.

2.5 STATIC FORCE CALIBRATOR

The deadweight force calibrator was used to statically calibrate both the electrodynamic actuator and the hybrid force measurement system.

The spatial orientation of the deadweight calibrator cable is coincident with the axis of the actuator armature to within ±0.001 in. The ±0.001-in. orientation accuracy is dictated by the specifications of the optical alignment equipment used during installation of the actuator and the deadweight calibrator. The in-place deadweight calibration of the load cell and the rest of the hybrid measurement circuitry obviates potential inaccurate force measurements caused by misalignment of the thrust butt mounted load cell and the rest of the force column.

The weights of the steel calibration plates were determined by a precision beam balance to within ± one gram.

SECTION III
PROCEDURE

3.1 CALIBRATION OF THE ACTUATOR AND THE HYBRID MEASUREMENT SYSTEM

3.1.1 Static Calibration

Deadweight of 14,128 gm was placed on the static calibrator cable. The actuator magnetic field current was set to 1.75 amp (current-regulated). Next, a d-c power supply was used to increase the current in the actuator armature (Fig. 2) until no net force was imparted to the load cell, as indicated by the voltage standard (Fig. 6). At this point in the calibration procedure, the developed force of the actuator just balanced the deadweight force. The voltage developed across the armature shunt, as indicated by digital voltmeter No. 1, was recorded as a calibration point. The d-c power supply was then disconnected, and the gain of the summing amplifier was adjusted until the reading of digital voltmeter No. 2 was identical to the previous reading of digital voltmeter No. 1. The 14,128-gm deadweight was then removed. The deadweights were next increased in 10 increments from zero to 28,128 gm, and the calibration points for the actuator were determined with the d-c power supply operative, whereas the static calibration points of the measurement system were determined with the d-c power supply inoperative. The static calibration data are shown in Fig. 7. This procedure caused the force measurement system scale factor, lb force/volt, to be equal to the actuator scale factor, lb force/volt. Equal scale factors permit direct determination of the instantaneous tracking error characteristics of the measurement system by direct comparison of the voltage signal across the armature shunt (armature current function determined by the current function generator) with the voltage signal at the output of the hybrid measurement system.

3.1.2 Dynamic Calibration

Next, the deadweight calibrator cable and d-c power supply were disconnected, and the current function generator was connected and activated. A fast rise time (0.6 msec) repetitive, 57-lb peak force was imparted to the force column. The armature shunt signal and hybrid measurement system output signal were superimposed on the oscilloscope, and the dynamic compensation adjustments were manipulated until the two signals were made to appear as identical as possible. An oscilloscope photograph was then taken to record the dynamic calibration data. The entire dynamic force calibration procedure, from activation of the current function generator through the recording of the oscilloscope photograph, required about two minutes.

It is estimated that oscilloscope presentation of the dynamic force calibration signal permits determination of the actual force to within two percent at the 50-lb force level. However, application of digital sampling techniques could permit determination of the actual force with an error of less than one percent.

The accuracy of dynamic force measurements with the hybrid system is directly dependent upon (1) the complexity of the thrust stand transient response characteristics, (2) the rise time of the input force, and (3) the degree to which the compensation technique is able to reconstruct the true force-time function. A fast rise time force imparted to a multidegree-of-freedom thrust stand presents a significantly more difficult compensation problem than does the excitation of a single-degree-of-freedom by a slow rise time force. The stand shown in Fig. 1 exhibits three significant amplitude natural frequencies -:390, 1670, and 3700 Hz. The instantaneous tracking error of this stand (using hybrid measurement techniques) at the 50-lb force level is as high as 100 percent during the first 200 μsec of the 0.6-msec rise time force but rapidly decreases to three percent within 4 msec after completion of the rise time portion of the force level change (see Section IV). The 100 percent tracking error figure would prevail for a finite length of time following a rapid force level change for any thrust measurement system since cause and effect phenomena in all physical systems are characterized by a time lag of the effect with respect to the cause. The 0.6-msec rise time force results in quite severe dynamic excitation of the stand, and the tracking error is correspondingly large. However, the instantaneous tracking error at the peak of a 5-msec rise time, 48-lb force is only 1.4 percent (see Section IV).

3.2 DYNAMIC COMPENSATION WITH THE SOLENOID EXCITER

The solenoid exciter shown in Fig. 4 was used to repetitively excite the natural frequencies of the experimental thrust stand shown in Fig. 1. The dynamic compensating adjustments of the electronic components shown in Fig. 6 were then accomplished so that the natural frequency distortions appearing in the measurement signal were eliminated as completely as possible.

3.2.1 Static Calibration

After completion of the dynamic compensation procedure, the entire hybrid force measurement system was subjected to a static force calibration using the electrodynamic actuator as a transfer standard. A direct

9

current was set into the armature circuit, and the shunt voltage as indicated by digital voltmeter No. 1 was recorded (Figs. 2 and 7). The gain of the summing amplifier (Fig. 6) was adjusted until the voltage indicated by digital voltmeter No. 2 was the same as voltmeter No. 1. This procedure caused the scale factor of the measurement system to be the same as that of the actuator. Direct photographic comparisons could then be made between force measurements made after actuator dynamic force calibration and after dynamic compensation with the solenoid exciter.

3.3 COMPARISON OF ACTUATOR AND IMPACT EXCITER DYNAMIC COMPENSATION AND FORCE CALIBRATION PROCEDURES

Two force-generating devices, the electrodynamic actuator and the solenoid exciter, have been used to dynamically excite the thrust stand structure. The instantaneous force delivered by the actuator is directly proportional to its armature current. The actuator output force-to-armature current shunt voltage was accurately determined by deadweight calibration. The introduction of dynamic forces with the actuator results in an actual dynamic force calibration.

The solenoid exciter used in the present study cannot be used as an actual dynamic force calibrator since it does not produce an electrical signal proportional to its impact force. In the present form the solenoid is used solely to excite the natural frequencies of the thrust stand structure so that the compensation circuitry can be properly adjusted. However, the use of a calibrated dynamic force gage as the impacting device would produce a signal proportional to the impact force, and it could, therefore, serve as a dynamic force calibrator.

The effectiveness of the solenoid exciter was evaluated by direct comparison of dynamic force data from the hybrid measurement system first dynamically force calibrated with the actuator and then dynamically compensated and statically force calibrated with the impact exciter and static force calibrator.

SECTION IV
RESULTS AND DISCUSSION

4.1 DYNAMIC FORCE CALIBRATION WITH THE ELECTRODYNAMIC ACTUATOR

Both the hybrid force measurement system and the electrodynamic actuator were statically calibrated with deadweight. The hybrid system gain was adjusted so that the scale factor, lb force/volt, was identical

to that of the actuator. The current function generator then was activated
to produce the periodic force-time function shown in Fig. 8a. From this
figure the force rise time is seen to be about 0.6 msec, and the peak
force is 57.2 lb ± 1.1 lb. The load cell signal, which is typical of the
conventional thrust stand output signal, was next superimpsoed upon the
force-time function, as shown in Fig. 8b. An expanded time scale photo-
graph of the data of Fig. 8b is shown in Fig. 8c. The maximum instan-
taneous tracking error of the load cell signal is seen to be about 70 percent.
The superimposed oscilloscope traces are furnished by a chopped input
vertical amplifier (chopper frequency - 1 MHz) so that the instantaneous
tracking error determinations are meaningful.

The next step in the dynamic force calibration procedure was adjust-
ment of the accelerometer signal gain and summation of this signal with
the load cell signal. The results of this summation are shown in Fig. 9a,
superimposed on the force-time function. An expanded time scale photo-
graph of the data of Fig. 9a is shown in Fig. 9b. It can be seen that the
390-Hz natural frequency distortion has been practically eliminated, but
the 1670-Hz natural frequency now distorts the measurement signal. The
appearance of the 1670-Hz distortion is due to the addition of the accel-
erometer signal. This is explainable by the fact that the output signal of
the accelerometer is the second time derivative of the load cell signal.
If the load cell signal is given by (assuming negligible damping):

$$V_{LC} = h_{LC} A \sin \omega_n t \qquad (2)$$

where V_{LC} is the load cell signal in volts, h_{LC} is the load cell scale
factor (volts/unit displacement across the load cell), A is the peak dis-
placement across the load cell, ω_n is the natural radian frequency and t
is time, then the accelerometer signal is given by:

$$V_A = - h_A A \omega_n^2 \sin \omega_n t \qquad (3)$$

where h_A is the accelerometer scale factor (volts/unit displacement/sec^2)
and V_A is proportional to the second time derivative of V_{LC}. From
Eq. (3) it can be seen that the accelerometer is more sensitive, by a
factor of ω_n^2, to natural frequency excitations then is the load cell.

One stage of computer compensation was next used to eliminate
the 1670-Hz distortion. The results of this step are shown in Fig. 10a.
An expanded time scale photograph of Fig. 10a is shown in Fig. 10b.
It can be seen that both the 390-Hz and the 1670-Hz distortions have
been practically eliminated. However, a small-amplitude 3700-Hz
distortion now appears in the measurement signal. Theoretically, the

3700-Hz distortion could be eliminated by another stage of computer compensation. An additional computer stage was not available at the time of this study, and further compensation could not be attempted.

A low-pass noise filter with a cutoff frequency of 6 KHz was placed before the computer compensator because of the differentiating characteristics of the compensator. The presence of the filter accounts for an appreciable amount of the time delay in the measurement system output signal. Relatively small time lags are also contributed by structural transportation lags and electronic system transit times. The time delay, plus the distortion effects of the uncompensated 3700-Hz natural frequency, accounts for the largest portion of the instantaneous tracking error during the rise time portion of the force-time function. This error is significantly smaller for slower rise time forces. This can be seen in Fig. 11 for a 5-msec rise time force. The instantaneous tracking error at the peak point of the 5-msec rise time is only about 1.4 percent.

Examination of Figs. 10a and 10b shows that some residual 390-Hz distortion still remains after all compensation adjustments have been completed. This distortion is caused by the damping action of the electrodynamic actuator as discussed in Section 2.2. This damping action causes the phase of the accelerometer signal with respect to the load cell signal to be other than the ideal 180 deg, and imperfect compensation of the 390-Hz distortion results. This problem is not met with the 1670-Hz distortion since damping characteristics are easily programmed into the computer compensator. It could be anticipated that the residual 390-Hz distortion would be greatly reduced during the actual rocket test since the actuator would be inoperative. The only effect to consider in regard to the use of the actuator is that the frequency of the predominant amplitude natural mode (usually the first mode for thrust stands) during the test would be slightly different from that for which the dynamic compensation adjustments were made. This could result in imperfect compensation adjustments. An estimate of this effect can be made by considering the relation between the damped and undamped natural frequency of a linear, time-invariant parameter, second-order system:

$$\omega_0 = \sqrt{1 - \zeta^2} \; \omega_n \qquad (4)$$

where ω_0 is the damped natural frequency, ω_n is the undamped natural frequency, and ζ is the damping ratio.

A serious compensation problem arises for certain solid-propellant rocket tests in which the solid-propellant mass is an appreciable fraction of the total force column mass. The natural frequencies of the force

column change during the test as mass is expended, and, in general, the compensation adjustments would have to be varied correspondingly throughout the test. However, if the particular rocket operates in a stable manner (free of large-amplitude combustion instabilities), possibly the only appreciable dynamic excitation during the test will occur during the thrust force rise time during which mass loss would be at a minimum and the compensation adjustments correct.

Soon after the data of Fig. 11 were recorded, the hybrid system output signal was found to be distorted by a natural frequency approximately that quoted by the manufacturer for the accelerometer resonant frequency. This distortion was later found to be caused by loosening of the accelerometer mount. This was unfortunate since the tracking error was slightly increased, and the inaccessibility of the accelerometer would have required disassembly of the entire stand if corrective action were to be taken. It was decided to continue the study in spite of the looseness of the accelerometer mount.

The data shown in Fig. 12 were recorded so that a comparison could be made with similar data derived from solenoid excitation and deadweight calibration. The measurement signal was superimposed upon the force-time function, as shown in Fig. 12a. Figure 12b is an expanded time scale photograph of Fig. 12a. Figure 12c is a presentation of the subtraction of the measurement signal from the force-time function and directly indicates the instantaneous error characteristics of the hybrid measurement system. The first peak in the data of Fig. 12c represents a force measurement error of about 14 lb and an instantaneous tracking error of about 100 percent. Close examination shows that this peak measurement error occurs during the measurement system delay time and is expected to be large. Four msec after the initiation of the force-time function, the instantaneous tracking error has decreased to three percent.

It should again be emphasized at this point that the data shown in Fig. 12 correspond to a 0.6-msec rise time force. Significant improvements in tracking error characteristics are noted for slower rise time forces.

4.2 DYNAMIC COMPENSATION WITH THE SOLENOID EXCITER

The solenoid exciter was next used to repetitively excite the natural frequencies of the stand so that the dynamic compensation circuitry could be adjusted. Figure 13a shows the load cell signal, and the 390-Hz distortion is evident. The data of Fig. 13b are the signal resulting

from the summation of the load cell and accelerometer signals. The 390-Hz distortion has been eliminated, but the 1670-Hz natural frequency now distorts the signal. Figure 13c shows the signal after compensation by the computer compensator. The 1670-Hz distortion has been eliminated, and the residual distortion is caused by the 3700-Hz natural frequency. The 3700-Hz distortion could have been eliminated had another stage of computer compensator circuitry been available. At this point the compensation procedure was complete; the entire procedure from initiation of the solenoid exciter through computer compensation required about two minutes.

4.2.1 Static Calibration

The electrodynamic actuator armature was next driven with a direct current until a 0.2-v shunt signal was recorded. The gain of the summing amplifier shown in Fig. 6 was adjusted so that digital voltmeter No. 2 read 0.2 v. This procedure set the measurement system scale factor equal to the actuator scale factor and completed the calibration procedure and constituted a static force calibration of the measurement system using the actuator as a transfer force standard.

The identical force-time function as recorded in Fig. 12 was again imparted to the thrust stand. The measurement signal is shown superimposed on the force-time function signal in Fig. 14a. Figure 14b is an expanded time scale photograph of Fig. 14a. Figure 14c is a photograph of the signal resulting from subtraction of the measurement signal from the force-time function. Perusal of Figs. 12 and 14 shows that the data of the two figures are essentially identical. The solenoid exciter in conjunction with a static force calibrator is thus seen to be as useful for dynamic force calibration as is the more complex and expensive electrodynamic actuator. Although the conclusion is based on the results obtained from a relatively low force rated (500-lb force maximum), horizontally oriented thrust stand, the same basic dynamic response problem is faced with smaller or larger thrust stands, whether oriented horizontally or vertically.

To determine the general applicability of the impact excitor-static force calibrator combination as a substitute for the electrodynamic actuator dynamic force calibrator, further comparisons should be made utilizing several different mechanically complex thrust stand structures.

SECTION V
SUMMARY OF RESULTS AND CONCLUSION

Two force-generating devices, an electrodynamic actuator and an impact exciter, were used to impart dynamic forces to an experimental thrust stand. A current shunt in the armature electrical circuit of the actuator produced a voltage proportional to the armature current and, therefore, also to the force produced by the actuator. The actuator output force to shunt voltage scale factor was accurately determined by deadweight calibration. This calibration remained valid for dynamic current level changes since the shunt inductance was only 0.15 μh, and inductive voltage drops were negligible. A current function generator was used to drive the armature of the actuator to produce a force-time function simulating rocket thrust buildup (0.6-msec rise time), burn time (35 msec), and tailoff (25-msec fall time). Determination of the actual force value from oscilloscope presentation of the force-time function was estimated to be possible within an error of two percent of the indicated peak force level of 57 lb (Ref. 4). While the actuator furnished periodic dynamic forces, the force measurement system dynamic compensation circuits were adjusted until the instantaneous tracking error was reduced to a minimum. This error was at a maximum during the rise time portion of the force-time function but rapidly decreased to its minimum value of three percent approximately 4 msec after initiation of the force-time function. The instantaneous tracking error characteristics were then recorded with an oscilloscope photograph. This photograph was later compared with a similar one of instantaneous tracking error characteristics (for the same force-time function) as a result of dynamic compensation circuit adjustments made possible by using the solenoid exciter. The photographs were found to be essentially identical, which shows that the calibration procedure using an impact-type dynamic force generator and static force calibrator is as valid as that using the electrodynamic actuator for the experimental thrust stand shown in Fig. 1.

The electrodynamic actuator and associated current function generator are quite complex mechanically and electronically as compared with an impact-type dynamic force generator. The alignment of the actuator armature with respect to its field structure is quite important since the clearance between the two is typically about 0.020 in. Therefore, the inclusion of an electrodynamic actuator adds significantly to the complexity of a thrust stand.

The dynamic response characteristics of the overall thrust stand, as influenced by the dynamic characteristics of any force calibrator, are of utmost importance. The instantaneous tracking error of any

thrust stand is directly related to the degree of success in eliminating the distortion effects of excited natural frequencies of the force column. An electrodynamic actuator armature is a relatively complex mechanical structure, and commercially available actuators may exhibit several resonances or natural frequencies. Compensation for three or possibly four natural frequencies is about a practical limit for the hybrid measurement technique so that inclusion of an electrodynamic actuator armature in a thrust stand force column could introduce several natural frequencies and contribute to the compensation problem. On the other hand, the impact-type dynamic force generator is not part of the thrust stand force column. This fact permits considerable mechanical simplification of the stand as compared with a stand incorporating an electrodynamic actuator. This mechanical simplification can in itself lead to a reduction in the number of force column natural frequencies to be encountered.

Complex thruster-thrust stand structures may require such a period of time for dynamic calibration that cooling of the electrodynamic actuator might have to be considered. Most commercially available actuators are forced air or convection cooled, and, unless other means are devised, radiation is the only cooling mechanism in the vacuum environment of the test cell. Impact-type force generators need only be afforded the same environment considerations as a conventional load cell.

The total cost of the small actuator, field power supply, and current function generator used in this study was a factor of 100 greater than the solenoid exciter and its control circuitry. The latter is inherently more reliable than the actuator system since it is rugged and simple, both mechanically and electronically.

The experimental data presented in Figs. 12 and 14 show that identical dynamic force measurement accuracies are obtained when using either the electrodynamic actuator dynamic force calibrator or the impact excitor-static force calibrator in conjunction with the experimental thrust stand shown in Fig. 1. However, further comparison tests with several different mechanically complex thrust stand structures should be conducted to determine the general applicability of the impact excitor-static force calibrator combination as a possible substitute for the electrodynamic actuator dynamic force calibrator. Also, tests should be conducted to determine the general applicability of a dynamic force gage or very stiff load cell as an impact-type dynamic force calibrator. An impacting force gage would furnish a signal accurately proportional to the impact force as long as its natural frequencies are not excited by the impact. Another quite important consideration for an impact-type dynamic force calibrator is the spatial orientation of the

impact force vector. Ideally, this vector should coincide with the force measurement axis of the thrust stand or at least be precisely defined. The precise specification of this vector could be a problem when the force gage impacts upon resilient materials.

A conceptual drawing of a thrust stand incorporating a dynamic force gage impact force calibrator is shown in Fig. 15. Hybrid dynamic compensation techniques would be used. The force gage can be detached from its mount for calibration purposes. The stress sensor of the gage could be the piezoresistive type.

A conceptual drawing of a vertically oriented stand for physically small solid-propellant rocket motors is shown in Fig. 16. The load cell could be statically calibrated before installation in the stand. However, a deadweight static force calibrator could quite easily be provided for this type of stand. In some cases a strain gage bridge, resistance unbalance-type static calibration would be adequate. Side force measurements and force gage impact-type dynamic force calibrators also could be provided.

A single-axis stand is shown in Fig. 15, but multiaxis dynamic force calibration could conceivably be accomplished by proper location of several impact-type dynamic force calibrators. Multiaxis dynamic force calibration with electrodynamic actuators would present a formidable design, installation and maintenance problem as compared with the use of dynamic force gages.

REFERENCES

1. Ward, J. S. "A System for Correcting for Spurious Natural-Frequency Ringing of Rocket Static Thrust Stands." U. S. Naval Ordnance Test Station NOTS TP-2541, NAVWEPS R-7569 (AD246982), China Lake, California, September 1960.

2. Postma, R. W. "Pulse Thrust Measuring Transducer." Rocketdyne Division of North American Aviation, Inc., Report No. R-6044, Canoga Park, California, January 1965.

3. Crosswy, F. L. and Kalb, H. T. "Investigation of Dynamic Rocket Thrust Measurement Techniques." AEDC-TR-67-202 (AD823181), November 1967.

4. Crosswy, F. L. and Kalb, H. T. "Evaluation of a Static and Dynamic Rocket Thrust Measurement Technique." AEDC-TR-68-117.

APPENDIX
ILLUSTRATIONS
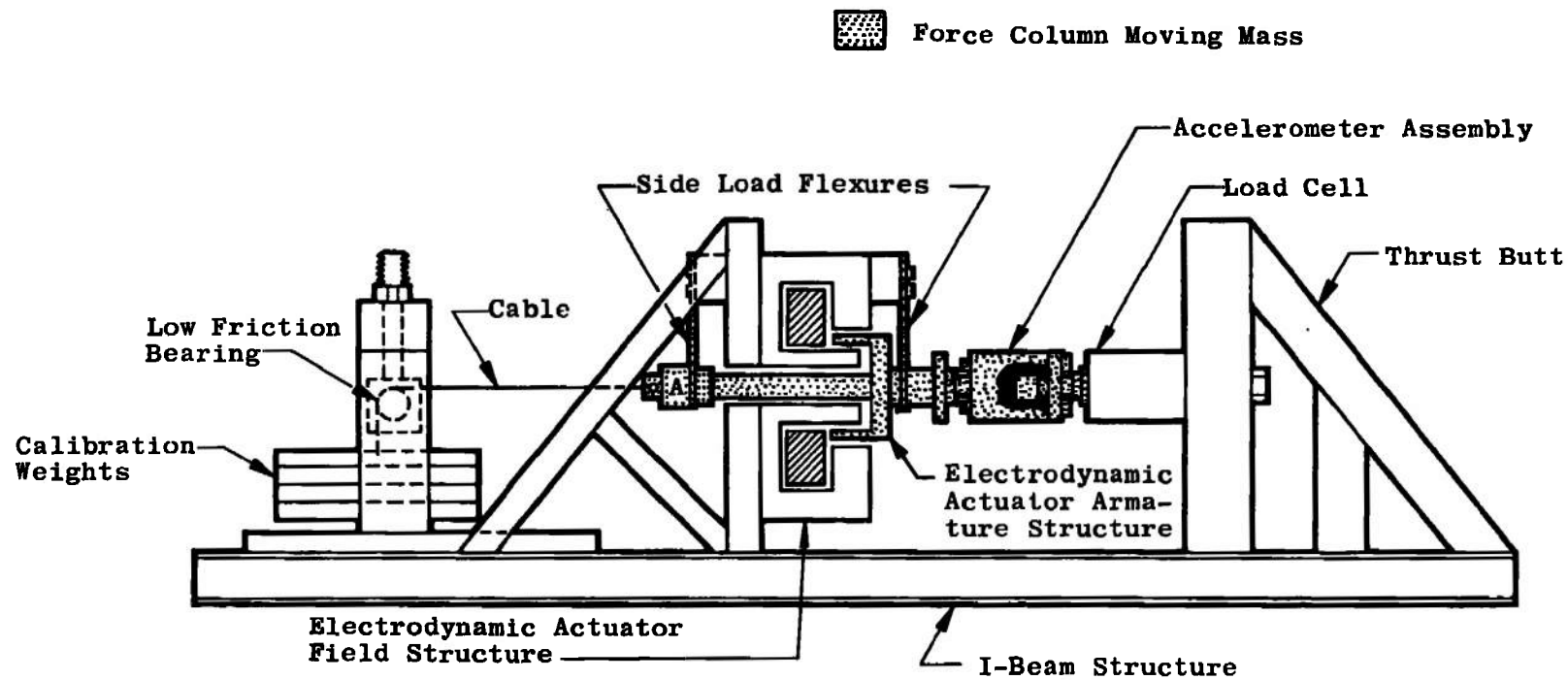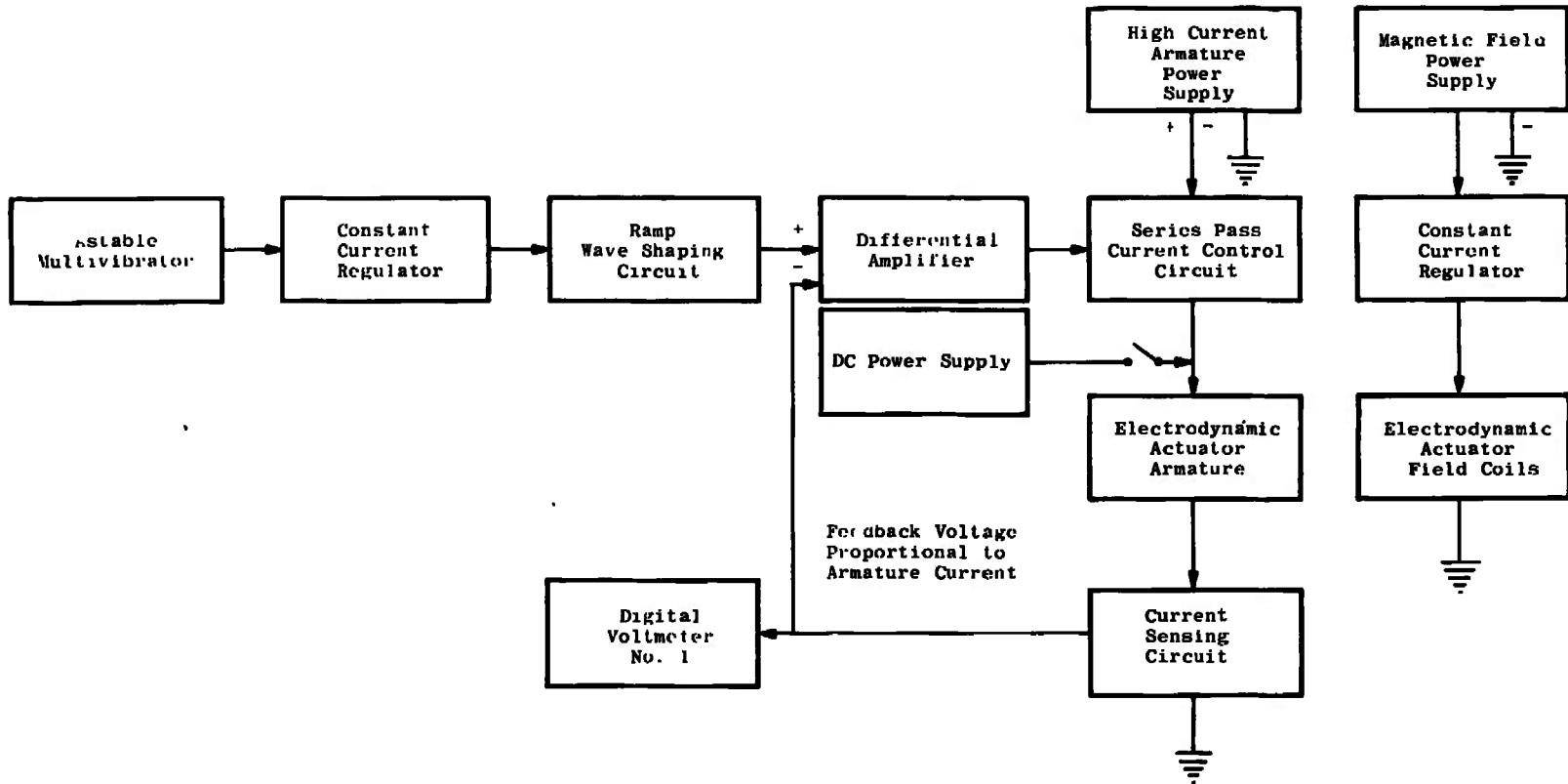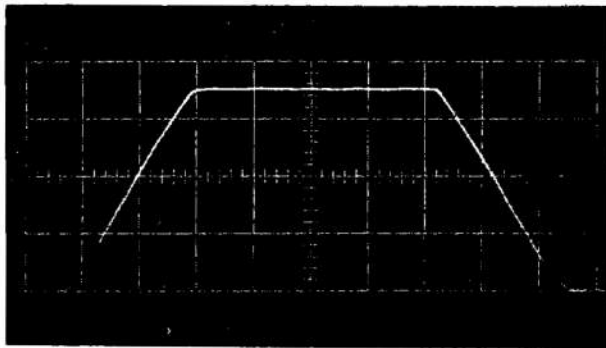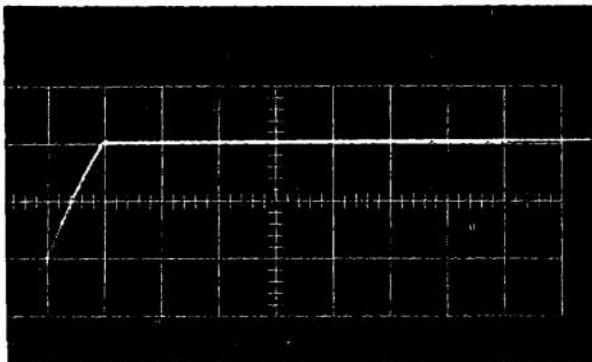
Fig. 1 Experimental Thrust Stand

Fig. 2 Block Diagram of Current Function Generator and Electrodynamic Actuator

Horizontal Scale - 10 msec/cm
Vertical Scale - 9338.8 gm/cm,
20.57 lb/cm

a. Dynamic Force Calibrator Peak Force — 32,688 gm, 72 lb

Horizontal Scale - 0.5 msec/cm
Vertical Scale - 4721.6 gm/cm,
10.4 lb/cm

b. Dynamic Force Calibrator Peak Force — 14,164.8 gm, 31.2 lb
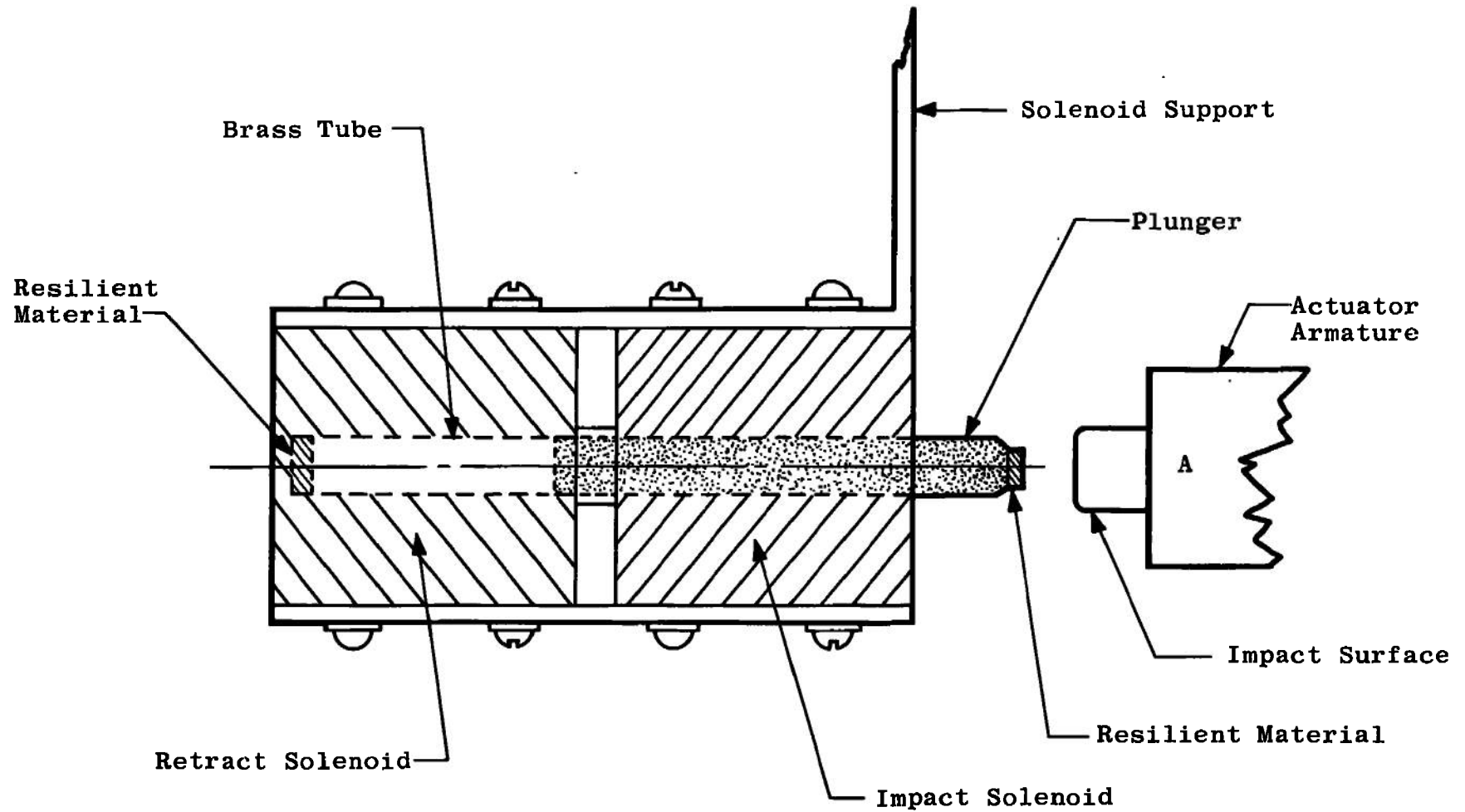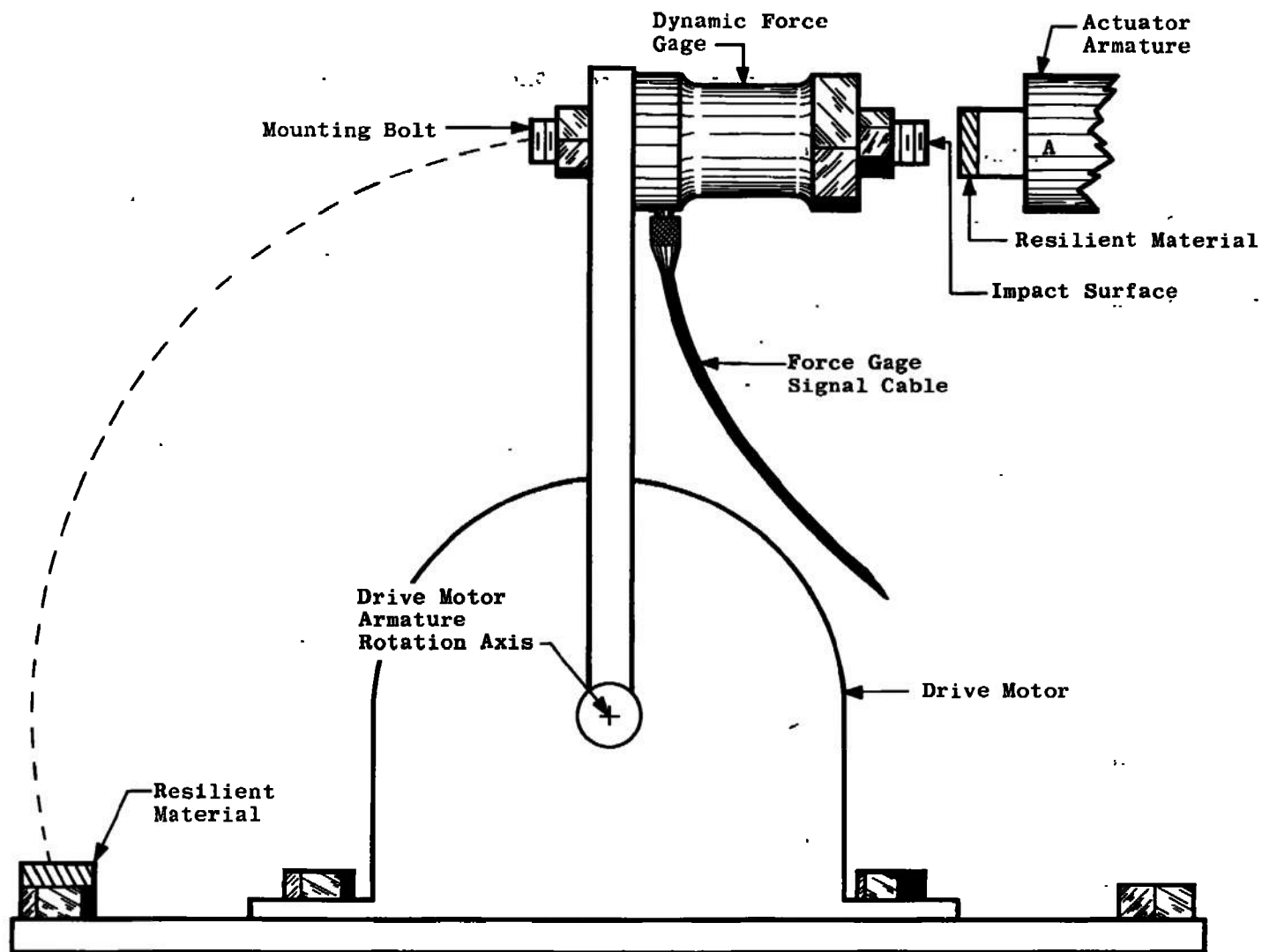Fig. 3 Typical Performance of the Current Function Generator

Brass Tube

Solenoid Support

Plunger

Resilient
Material

Actuator
Armature

A

Impact Surface

Retract Solenoid

Resilient Material

Impact Solenoid

Fig. 4 Solenoid Exciter

Dynamic Force Gage

Actuator Armature

Mounting Bolt

A

Resilient Material

Impact Surface

Force Gage Signal Cable

Drive Motor Armature Rotation Axis

Drive Motor

Resilient Material

Fig. 5 Force Gage Impact Device
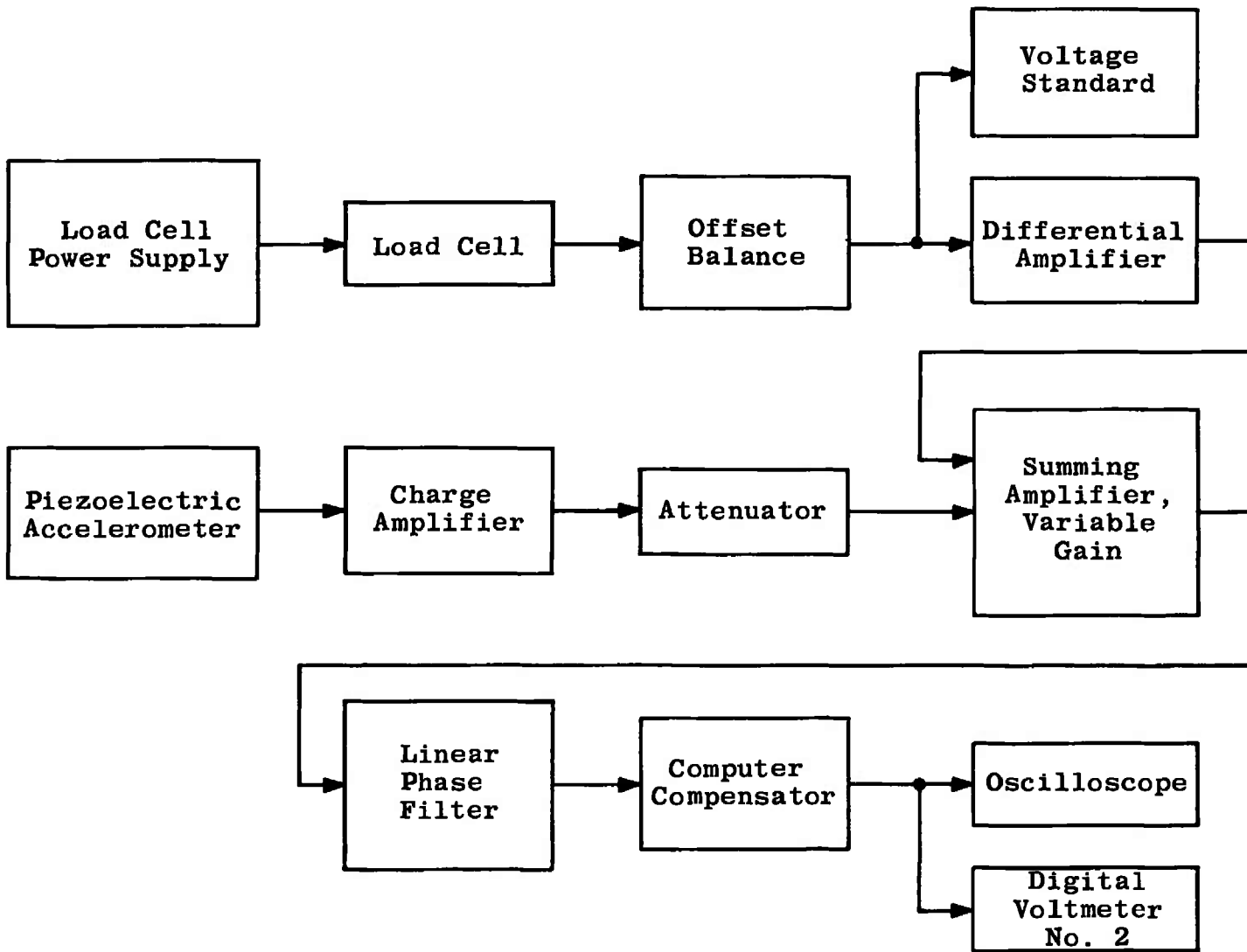
Fig. 6 Block Diagram of Hybrid System Transducers and Electronic Components
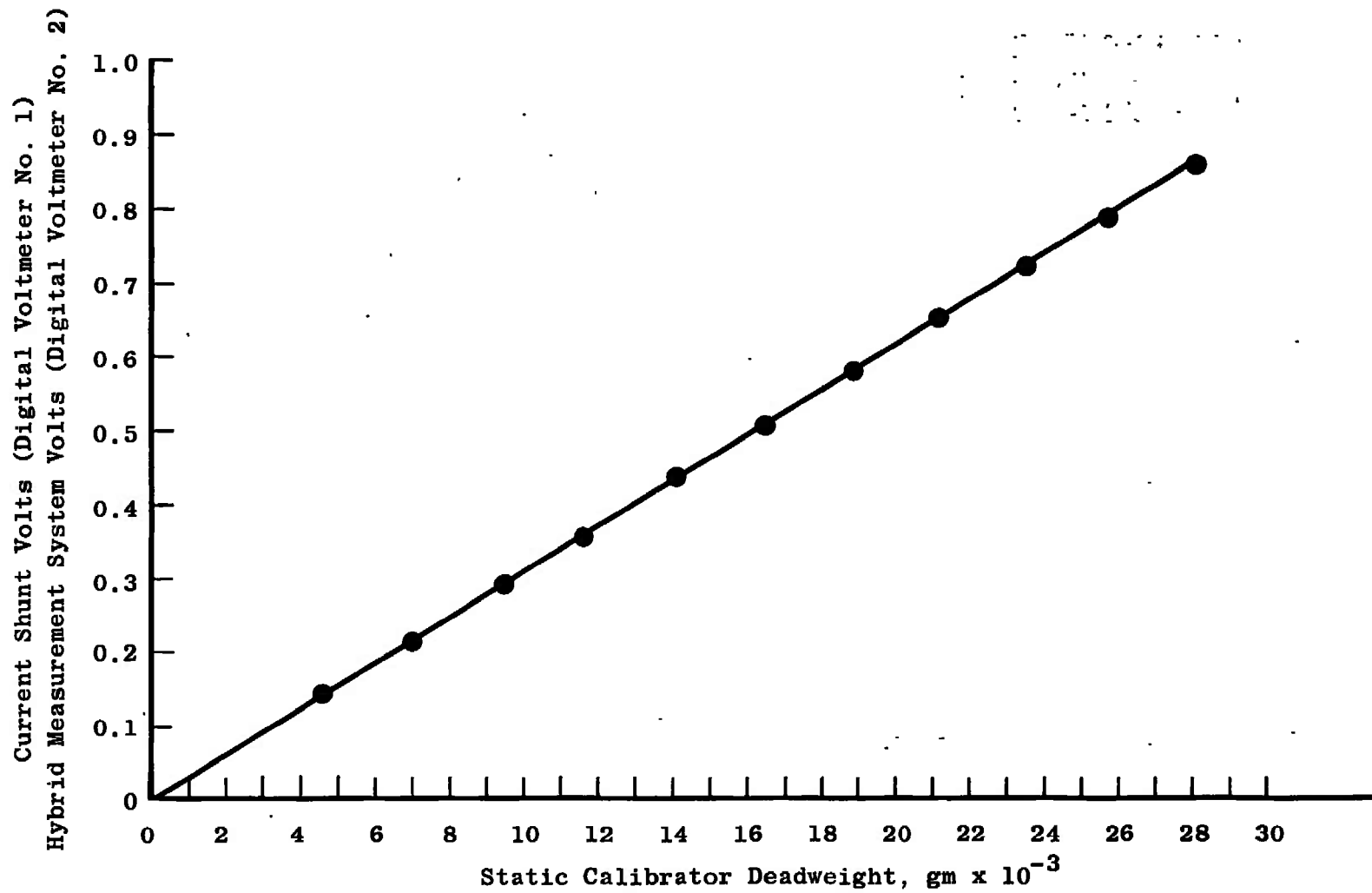
Fig. 7 Electrodynamic Actuator and Hybrid Measurement System Static Force Calibration
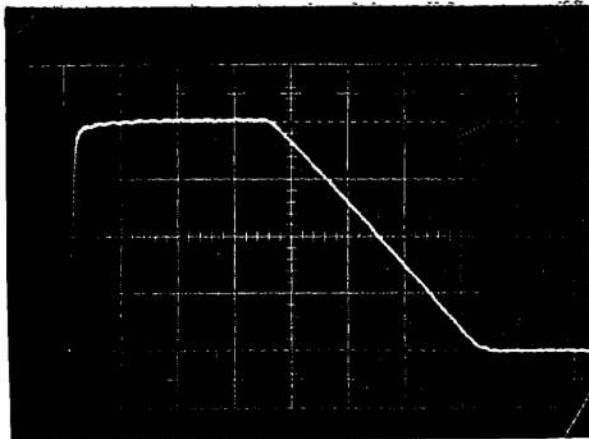
Horizontal Scale - 10 msec/cm
Vertical Scale - 6500 gm/cm,
                         14.32 lb/cm
Calibrator Peak Force -
26,000 gm, 57.26 lb

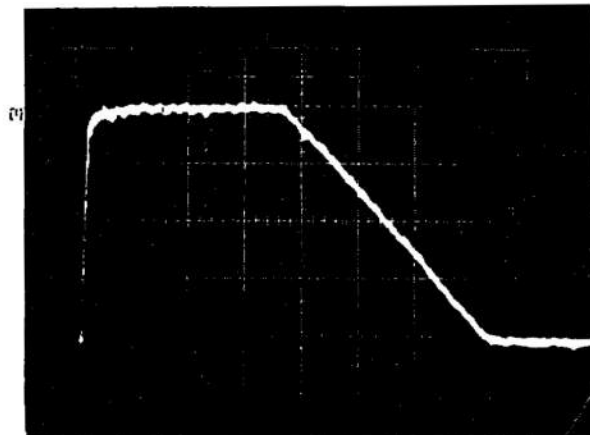a. Dynamic Force Calibrator Force-Time Function
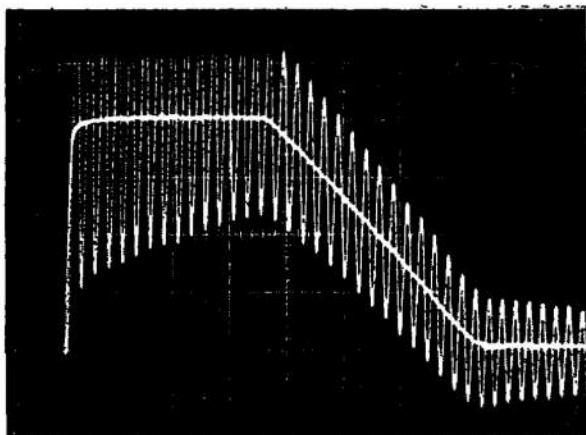
Horizontal Scale - 10 msec/cm
Vertical Scale - 6500 gm/cm,
                         14.32 lb/cm
Calibrator Peak Force -
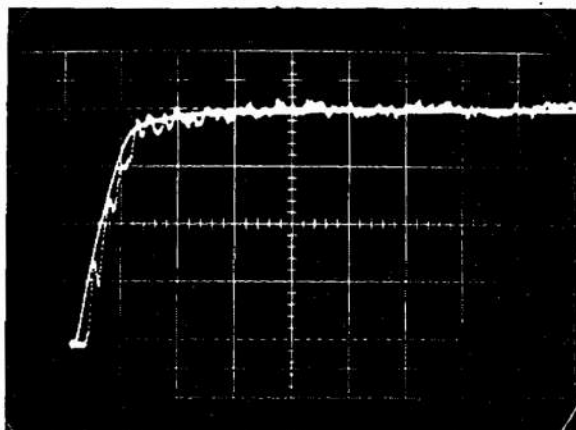26,000 gm, 57.26 lb

b. Load Cell Response Superimposed on the Force-Time Function

Fig. 8 Electrodynamic Actuator Dynamic Force Calibration Sequence-Load Cell Signal
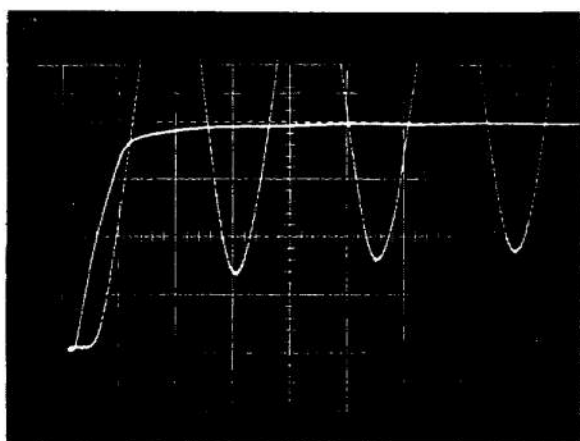
Horizontal Scale – 1 msec/cm
Vertical Scale – 6500 gm/cm,
14.32 lb/cm
Calibrator Peak Force –
26,000 gm, 57.26 lb

c. Expanded Time Scale Photograph of Fig. 8b

Fig. 8 Concluded
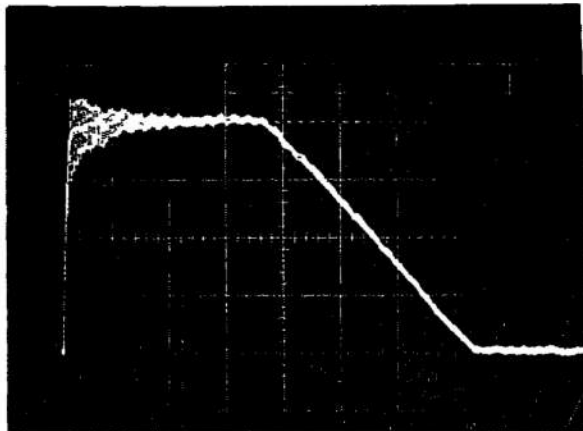
Horizontal Scale - 10 msec/cm
Vertical Scale - 6500 gm/cm,
                 14.32 lb/cm
Calibrator Peak Force -
26,000 gm, 57.26 lb

a.   Reaction Force Summation Signal Superimposed on the Force-Time Function
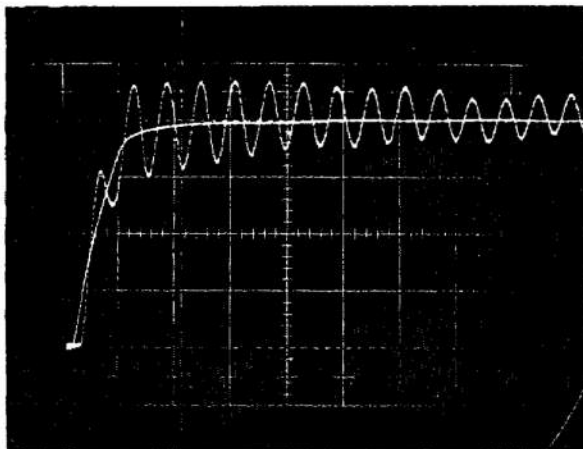
Horizontal Scale - 1 msec/cm
Vertical Scale - 6500 gm/cm,
                 14.32 lb/cm
Calibrator Peak Force -
26,000 gm, 57.26 lb

b.   Expanded Time Scale Photograph of Fig. 9a

Fig. 9   Electrodynamic Actuator Dynamic Force Calibration Sequence-Reaction Force Summation Signal

Horizontal Scale - 10 msec/cm
Vertical Scale - 6500 gm/cm,
                        14.32 lb/cm
Calibrator Peak Force -
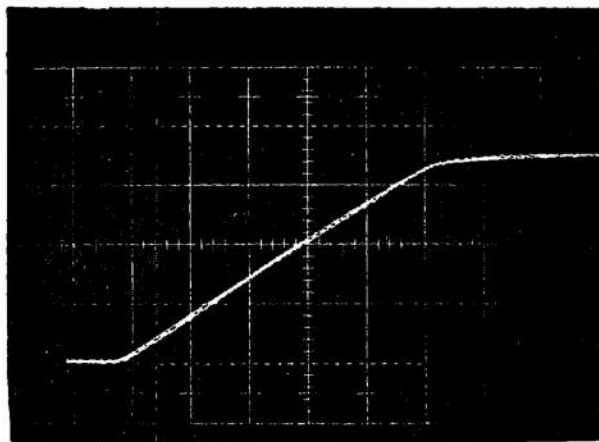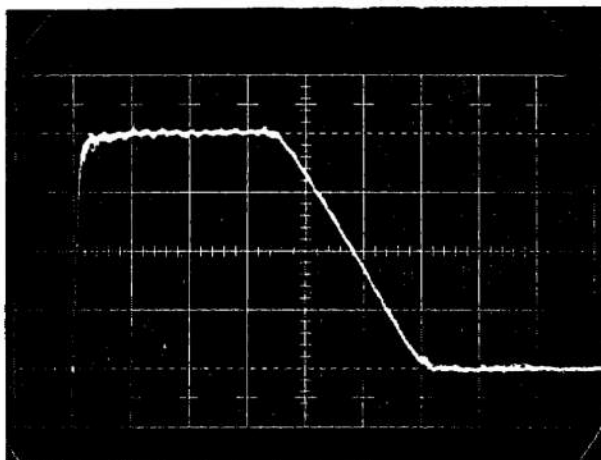26,000 gm, 57.26 lb

a. Hybrid System Signal Superimposed on the Force-Time Function

Horizontal Scale - 1 msec/cm
Vertical Scale - 6500 gm/cm,
                        14.32 lb/cm
Calibrator Peak Force -
26,000 gm, 57.26 lb

b. Expanded Time Scale Photograph of Fig. 10a
Fig. 10 Electrodynamic Actuator Dynamic Force Calibration Sequence-Hybrid System Signal

31

Horizontal Scale - 1 msec/cm
Vertical Scale - 6500 gm/cm,
                 14.32 lb/cm
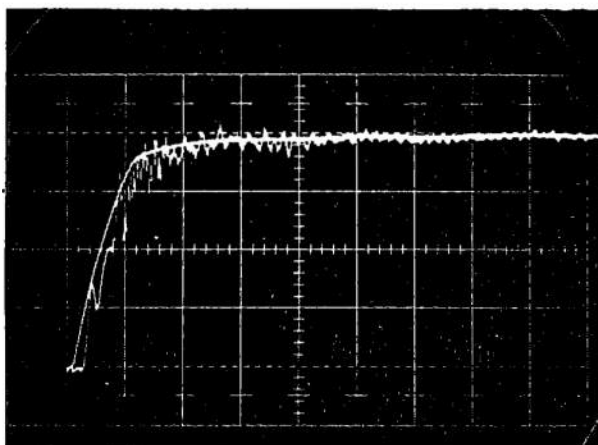Calibrator Peak Force -
22,230 gm, 48.97 lb

Fig. 11 Instantaneous Tracking Error Characteristics for 5-msec Rise Time Force-Time Function

Horizontal Scale - 10 msec/cm
Vertical Scale - 6500 gm/cm,
                        14.32 lb/cm
Calibrator Peak Force -
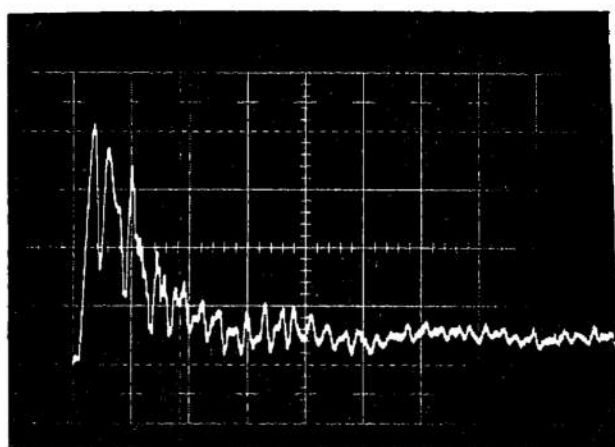26,000 gm, 57.26 lb

a. Hybrid System Signal Superimposed on the Force-Time Function

Horizontal Scale - 1 msec/cm
Vertical Scale - 6500 gm/cm,
                        14.32 lb/cm
Calibrator Peak Force -
26,000 gm, 57.26 lb

b. Expanded Time Scale Photograph of Fig. 12a

Fig. 12 Instantaneous Tracking Error Characteristics following Electrodynamic
Actuator Dynamic Force Calibration

Horizontal Scale – 1 msec/cm
Vertical Scale – 1625 gm/cm,
3.58 lb/cm
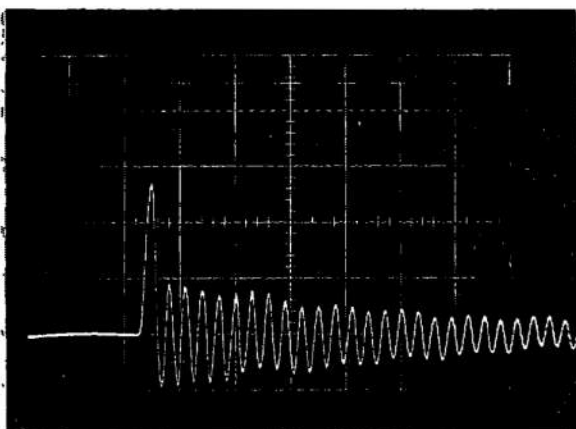Maximum Force Measurement
Error – 6775 gm, 14.93 lb

c. Subtraction of Hybrid System Measurement Signal from the Dynamic Force
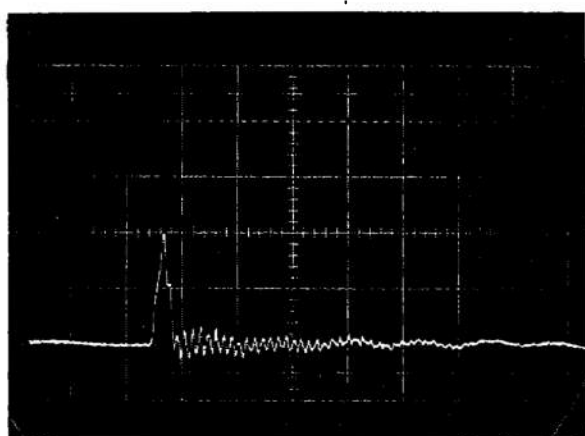Calibrator Force-Time Function Signal
Fig. 12 Concluded
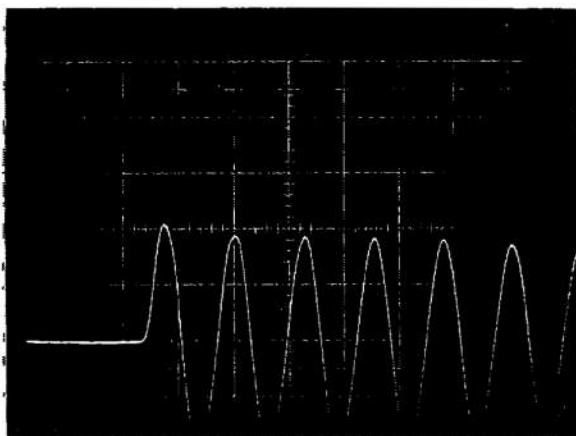
Horizontal Scale - 2 msec/cm
Vertical Scale - Not Calibrated

a. Load Response to Exciter Impact

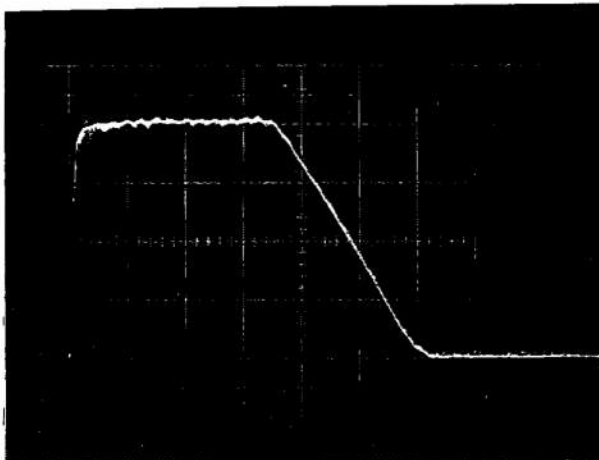Horizontal Scale - 2 msec/cm
Vertical Scale - Not Calibrated

b. Reaction Force Summation Response to Exciter Impact
Fig. 13 Solenoid Exciter Dynamic Compensation Sequence

Horizontal Scale - 2 msec/cm
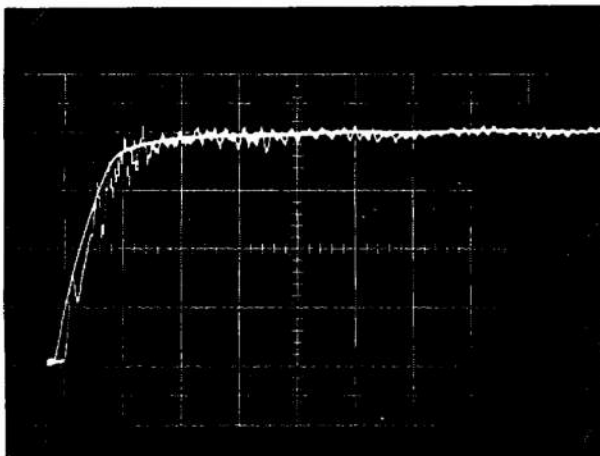Vertical Scale - Not Calibrated

c. Hybrid System Response to Exciter Impact

Fig. 13 Concluded

Horizontal Scale - 10 msec/cm
Vertical Scale - 6500 gm/cm,
                 14.32 lb/cm
Calibrator Peak Force -
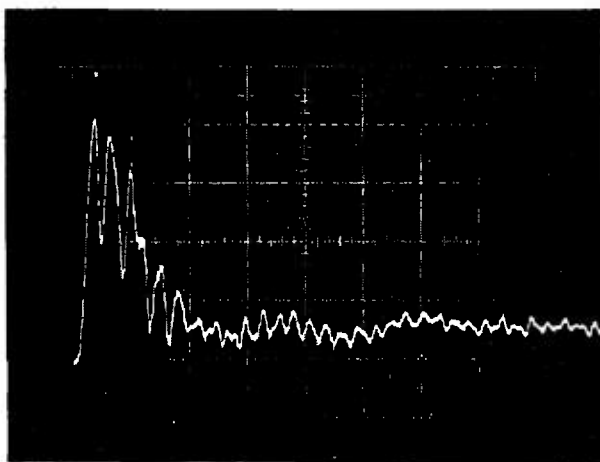26,000 gm, 57.26 lb

a. Hybrid System Signal Superimposed on the Force-Time Function

Horizontal Scale - 1 msec/cm
Vertical Scale - 6500 gm/cm
                 14.32 lb/cm
Calibrator Peak Force -
26,000 gm, 57.26 lb

b. Expanded Time Scale Photograph of 14a

Fig. 14 Instantaneous Tracking Error Characteristics following Solenoid Exciter
Dynamic Compensation and Deadweight Calibration

Horizontal Scale - 1 msec/cm
Vertical Scale - 1625 gm/cm,
          3.58 lb/cm
Maximum Force Measurement
Error - 6775 gm, 14.93 lb

c. Subtraction of Hybrid System Measurement Signal from the Dynamic Force
   Calibrator Force-Time Function Signal

Fig. 14 Concluded

Thrust Butt Brace

Load Cell

Thrust Butt

Accelerometer

Static Calibrator
Pull Rods (2)

Pull Rod Engaging Device

Rocket Engine

Automatic
Deadweight
Loading Device

Support Flexure

Force
Gage

Drive
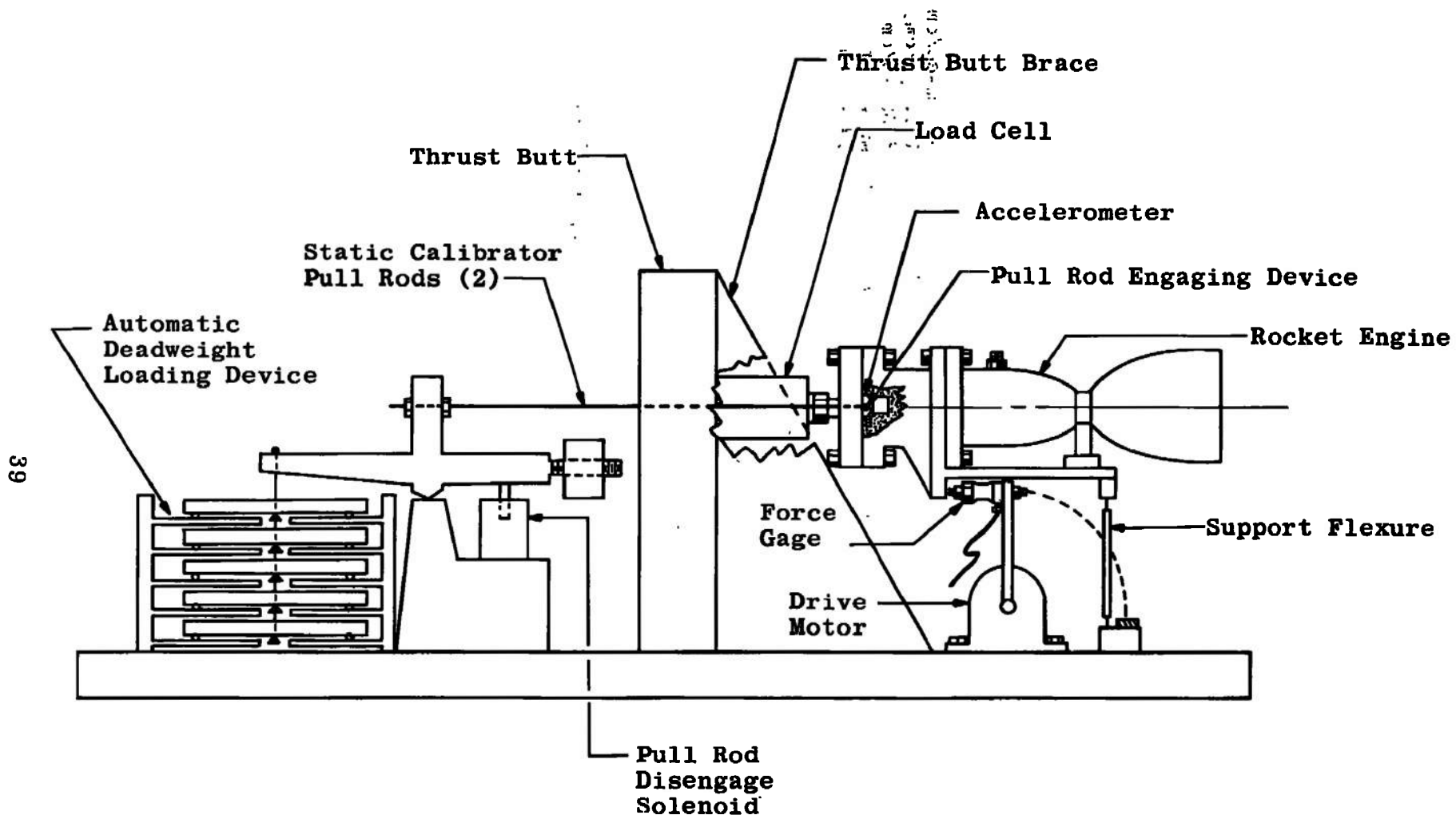Motor

Pull Rod
Disengage
Solenoid

Fig. 15 Horizontally Oriented Thrust Stand with an Impact-Type Dynamic Force Calibrator
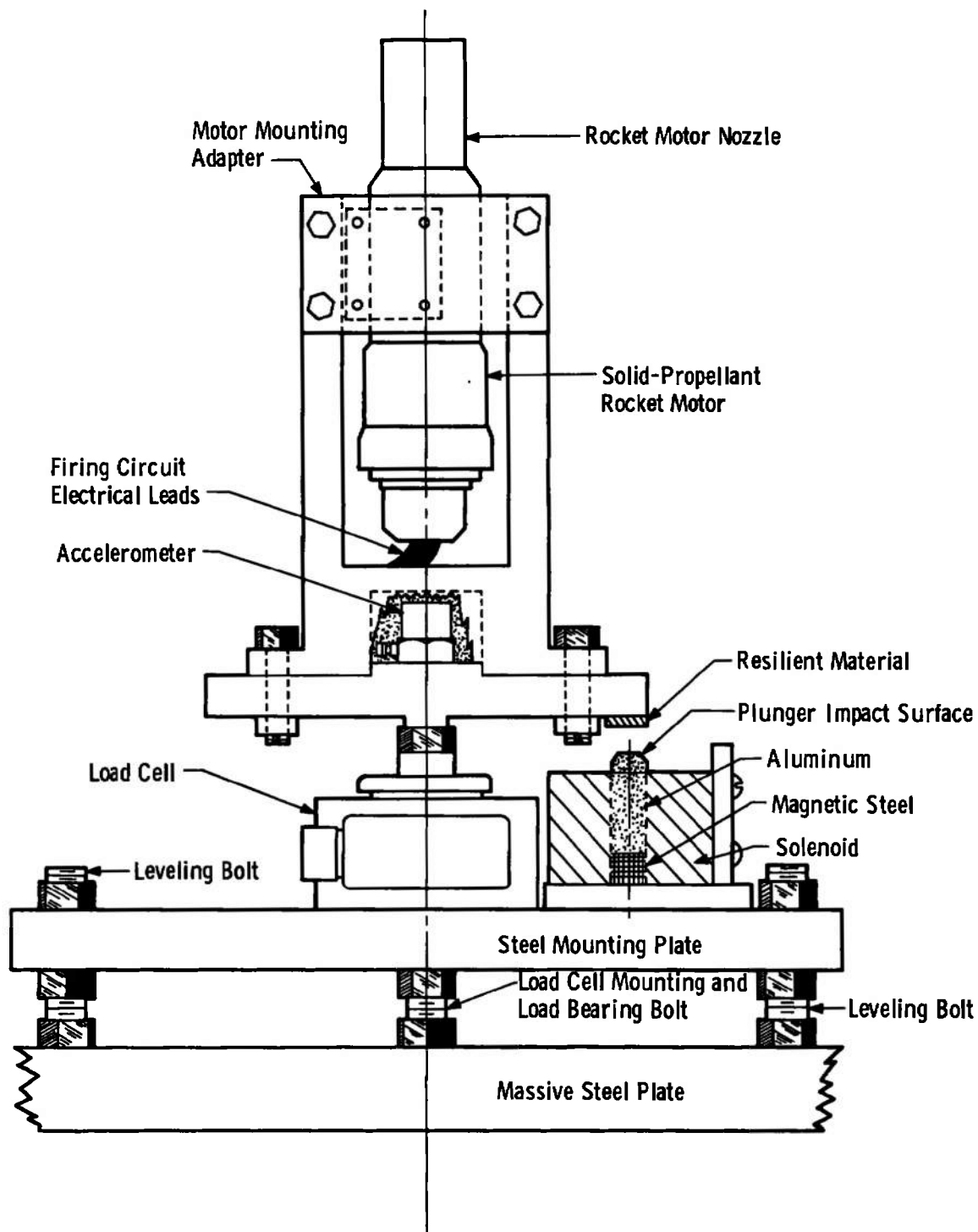
Fig. 16 Vertically Oriented Thrust Stand with a Solenoid Exciter

DOCUMENT CONTROL DATA - R & D

(Security classification of title, body of abstract and indexing annotation must be entered when the overall report is classified)

1. ORIGINATING ACTIVITY *(Corporate author)*	2a. REPORT SECURITY CLASSIFICATION
Arnold Engineering Development Center ARO, Inc., Operating Contractor Arnold Air Force Station, Tennessee	UNCLASSIFIED
	2b. GROUP
	N/A

3. REPORT TITLE

DYNAMIC COMPENSATION AND FORCE CALIBRATION TECHNIQUES FOR A
STATIC AND DYNAMIC THRUST MEASUREMENT SYSTEM

4. DESCRIPTIVE NOTES *(Type of report and inclusive dates)*
June to August 1967 – Final Report

5. AUTHOR(S) *(First name, middle initial, last name)*

F. L. Crosswy and H. T. Kalb, ARO, Inc.

6. REPORT DATE	7a. TOTAL NO. OF PAGES	7b. NO. OF REFS
November 1968	47	4

8a. CONTRACT OR GRANT NO.	9a. ORIGINATOR'S REPORT NUMBER(S)
F40600-69-C-0001	
b. PROJECT NO. 5730	AEDC-TR-68-202
c. Program Element 62302F	9b. OTHER REPORT NO(S) *(Any other numbers that may be assigned this report)*
d. Task 04	N/A

10. DISTRIBUTION STATEMENT

This document has been approved for public release and sale;
its distribution is unlimited.

11. SUPPLEMENTARY NOTES	12. SPONSORING MILITARY ACTIVITY
Available in DDC	Arnold Engineering Development Center, Air Force Systems Command, Arnold Air Force Station, Tennessee

13. ABSTRACT

An electrodynamic actuator and a solenoid-driven impact device were
used separately for dynamic force excitation of an experimental thrust
stand. Electronic compensation techniques were used to eliminate load
cell signal distortions caused by the dynamic-force-induced transient
response characteristics of the thrust stand structure. It was deter-
mined that proper compensation circuit adjustments could be made when
using either the electronically and mechanically simple impact device
or the more complex actuator. For the conditions of this particular
study, identical dynamic force measurement accuracies were possible
following either of two procedures, (1) dynamic time domain force cali-
bration with the electrodynamic actuator or (2) dynamic compensation
adjustments with dynamic force excitation furnished by the impact device
followed by a static deadweight force calibration.

14. KEY WORDS	LINK A		LINK B		LINK C	
	ROLE	WT	ROLE	WT	ROLE	WT
thrust						
measurement						
electrodynamics						
actuators						
impact						
force						
test equipment						
solenoids						